JACS
JOURNAL OF THE AMERICAN CHEMICAL SOCIETY

ARTICLE

pubs.acs.org/JACS

Nature of Electron Transport by Pyridine-Based Tripodal Anchors: Potential for Robust and Conductive Single-Molecule Junctions with Gold Electrodes

Yutaka Ie,[†,‡] Tomoya Hirose,[†] Hisao Nakamura,[*,#] Manabu Kiguchi,[*,§] Noriaki Takagi,[∥] Maki Kawai,[∥,⊥] and Yoshio Aso[*,†]

[†]The Institute of Scientific and Industrial Research (ISIR), Osaka University, 8-1, Mihogaoka, Ibaraki, Osaka 567-0047, Japan

[‡]PRESTO-JST, 4-1-8, Honcho, Kawaguchi, Saitama 333-0012, Japan

[#]Nanosystem Research Institute (NRI) "RICS", National Institute of Advanced Industrial Science and Technology (AIST), Central 2, Umezono 1-1-1, Tsukuba, Ibaraki 305-8568, Japan

[§]Department of Chemistry, Graduate School of Science and Engineering, Tokyo Institute of Technology, 2-12-1 W4-10, Ookayama, Meguro-ku, Tokyo 152-8551, Japan

[∥]Department of Advanced Materials Science, The University of Tokyo, Kashiwa, Chiba 277-8561, Japan

[⊥]Surface Chemistry Laboratory, RIKEN, Wako, Saitama 351-0198, Japan

Supporting Information

ABSTRACT: We have designed and synthesized a pyridine-based *tripodal* anchor unit to construct a single-molecule junction with a gold electrode. The advantage of tripodal anchoring to a gold surface was unambiguously demonstrated by cyclic voltammetry measurements. X-ray photoelectron spectroscopy measurements indicated that the π orbital of pyridine contributes to the physical adsorption of the tripodal anchor unit to the gold surface. The conductance of a single-molecule junction that consists of the tripodal anchor and diphenyl acetylene was measured by modified scanning tunneling microscope techniques and successfully determined to be $5 \pm 1 \times 10^{-4}$ G_0. Finally, by analyzing the transport mechanism based on ab initio calculations, the participation of the π orbital of the anchor moieties was predicted. The tripodal structure is expected to form a robust junction, and pyridine is predicted to achieve π-channel electric transport.

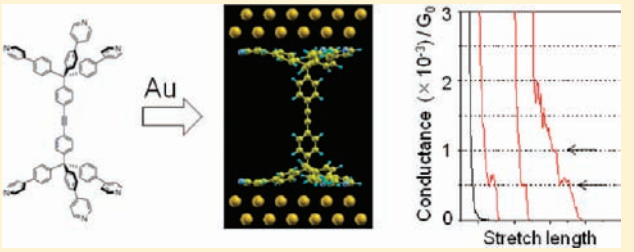

INTRODUCTION

Developing functional organic electronic devices is one of the most active research fields in nanoscience.[1] For instance, there are several candidate devices in nanoelectronics, nanofabrication (dense nanowire),[2] and nanomaterial electronics (carbon nanotube, graphene).[3] Single-molecule electronics are also one of the promising candidates in terms of ultimate miniaturization. They have a number of potential advantages for constructing functional devices, primarily because a great variety of molecules and their flexible conformations enable the design of various functionalities.[4] For instance, the first proposal of a molecular device was introduced by Aviram and Ratner, who focused on the function of molecular rectification by designing donor−acceptor linked molecules.[5] Given that the advantage of molecular electronics relies on varieties of molecules and their fine-tuned properties, chemistry should play a key role in designing and synthesizing functional electric materials using the encyclopedic methodological knowledge base of organic synthetic chemistry. In this sense, clarifying the relationships between "molecular properties" and their "device characters" is one of the central issues for developing molecular electronics as well as fabricating practical molecular devices.

However, realization of a practical single-molecule device requires reliable contact between the bridging molecule and the electrodes, where sufficiently strong binding between two terminal anchoring groups of the bridging molecule and the metal electrodes is achieved.[6] In this context, scanning tunneling microscopy (STM), conducting atomic force microscopy (AFM), and mechanically controllable break junctions (MCBJ) are now established as standard techniques to form the contact; they have been extensively investigated to measure the conductance of many metal−molecule−metal junctions.[7] Hence, selection of the proper anchoring group is quite important in creating the junctions. An anchoring group should satisfy the following conditions. It should (i) form sufficiently strong connections between a molecule and metal surfaces, and (ii) maintain sufficient electron density of states (DOS) close to the Fermi

Received: October 25, 2010
Published: February 10, 2011

level to pass an electron or hole through the molecule. Furthermore, in order to design tailor-made functional devices, it must be able to (iii) control well-ordered molecular orientations.

As a simple strategy, a single point (region) can be designated on each electrode as the "anchoring point," where the connection is formed by σ-bond formation (e.g., thiol (SH),[8] selenol (SeH)[9,10]), or physical adsorption (e.g., amine (NH_2),[8,11] pyridine[7,12−15]) between functional groups and noble metal electrodes. Recently, a different anchoring strategy utilizing direct hybridization of the π orbital of a conjugated molecule (e.g., benzene,[16] fullerene,[17] etc.) and the metal has been examined, with high conductance values of single-molecule junctions reported by several groups. This hybridization behavior is quite similar to the case of the interface between an organic semiconductor film such as 3,4,9,10-perylenetetracarboxylic dianhydride (PTCDA) film and a metal surface such as silver.[18] However, there are still limits to extending this strategy to design new anchoring units, especially for application to single-molecule junctions, that satisfy all three requirements above.

One reason for the difficulty of anchoring the molecule while maintaining an ordered molecular orientation is that the anchoring point is spatially limited and/or a single molecule can slide in parallel to the electrode (tip) surface. Hence, the use of a tripodal structure has been proposed by several groups.[10,19−22] We have demonstrated that the tripodal structure contributes not only to maintaining the robustness of surface attachment but also to controlling the molecular orientation.[10,21] However, to the best of our knowledge, there are no measurements of electrical conductance for a single molecule bearing tripodal anchoring groups.

In the present study, we have examined the possibility of a "conductive" molecular junction connected by tripodal anchors, which can be expected to satisfy the conditions of robustness of adsorption and well-ordered orientation. Recently, conductance measurements of simple bipyridine junctions were reported,[7,12a,12e] and a transport mechanism based on π−metal interactions was proposed.[13] Hence, we adopt pyridine as a candidate anchoring group in the tripodal structure, as shown in Figure 1. Here, the notations **Py** and **PE** represent the pyridine and diphenylene-ethynylene groups, respectively. We labeled the tripodal structure of the pyridine as **3Py**. We report a comprehensive study toward a single-molecule device. Specifically, we report the synthesis of **3Py-TIPS**, **3Py-Ph4T**, and **3Py-PE-3Py**, the formation of **3Py-TIPS** and **3Py-Ph4T** monolayers and their evaluations by electrochemical measurements and X-ray photoelectron spectroscopy (XPS), and subsequently the measurements of single-molecule conductance for **3Py-PE-3Py**. Furthermore, we analyze the potential of our newly developed pyridine tripodal structure as an anchor for molecular devices using ab initio transport calculations.

RESULTS AND DISCUSSION

Synthesis. The target compounds **3Py-TIPS**, **3Py-Ph4T**, **3Py-PE-3Py**, and the reference compound **1Py-Ph4T**, were synthesized using the Suzuki, Sonogashira, and Stille coupling reactions (Scheme 1). Phenyl-capped oligothiophene (**Ph4T**) was introduced as an active component for cyclic voltammetry (CV) measurements. The target compounds, being soluble in common organic solvents such as chloroform, were thus successfully purified by gel-permeation liquid chromatography. These compounds were unambiguously characterized by nuclear magnetic resonance (NMR) spectroscopy, mass spectroscopy (MS),

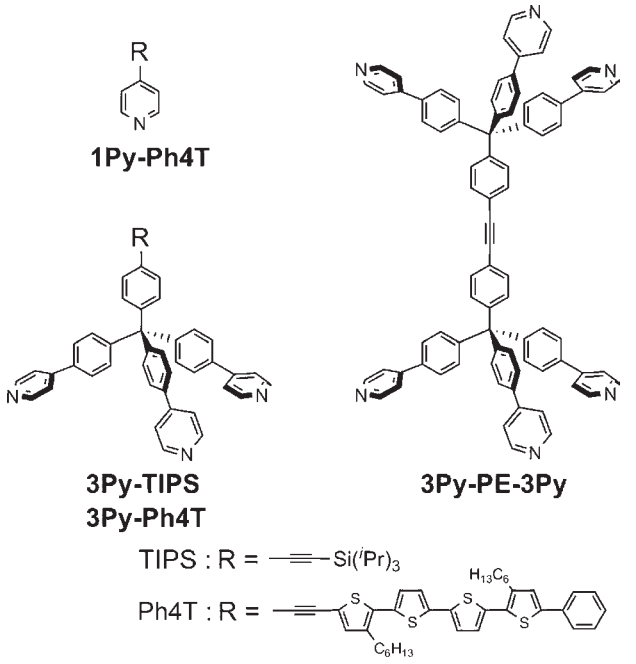

Figure 1. Chemical structures.

and elemental analysis. The synthetic details and compound-identification data are summarized in the Experimental Section.

Evaluation of Monolayers. Monolayers of **3Py-Ph4T** and **1Py-Ph4T** were prepared by immersing Au-on-mica substrates in their dichloromethane solution (5.0×10^{-4} M) for 12 h. The electrochemical properties of the monolayers were investigated by CV measurements, which were carried out at a scan rate of 100 mV s^{-1} in dichloromethane containing 0.1 M tetrabutylammonium hexafluorophosphate ($TBAPF_6$) as a supporting electrolyte using the monolayer-modified gold as a working electrode, platinum wire as a counter electrode, and $Ag/AgNO_3$ as a reference electrode. As shown in Figure 2a, CVs with the **3Py-Ph4T**-modified gold electrodes displayed a reversible one-electron redox wave that corresponds to the oxidation process of the **Ph4T** moiety. The surface coverage of the adsorbed molecules was estimated to be 7.1×10^{-11} mol cm^{-2} by integrating the anodic peak area. On the other hand, **1Py-Ph4T**-modified electrodes did not show any corresponding redox wave under the same measurement conditions, indicating that **1Py-Ph4T** has a weak tendency to be adsorbed on gold in comparison with **3Py-Ph4T**. This difference can be explained by the multiplier effect of the pyridyl tripodal structure. It is important to note that the electrochemical response (surface coverage) of the monolayer **3Py-Ph4T** remains at 30% of the original value after 10 scans within the range of 0−0.55 V (Figure 2b and Figure S1). This indicates that robust junctions, which are indispensible for the fabrication of molecular devices, were formed.

To obtain insight into the **3Py-TIPS**-adsorbed state, XPS measurements were performed at room temperature in an ultrahigh vacuum chamber. As shown in Figure 3, the XPS spectrum exhibits a peak at 399.4 eV, corresponding to N 1s.[23] It has been reported that the perpendicular geometry of the pyridine ring on the gold surface causes interactions to occur between the gold and nitrogen atoms, leading to the detection of a positively charged nitrogen peak at around 402 eV in addition to the characteristic N 1s peak.[24] However, such a peak is not observed in our measurements. This suggests that parallel

Scheme 1[a]

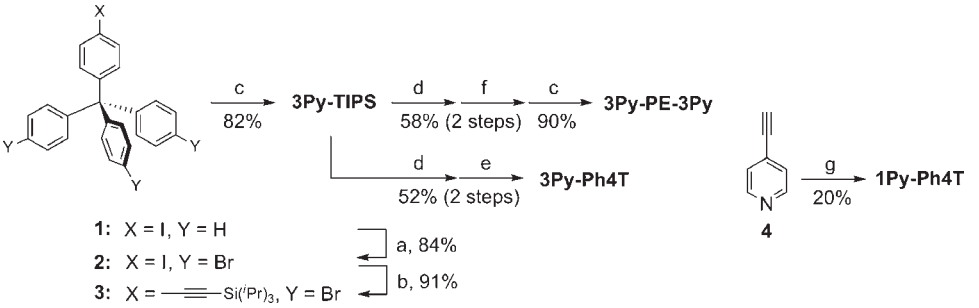

[a] Reagents and conditions: (a) Br_2, CH_2Cl_2, r.t.; (b) $PdCl_2(PPh_3)_2$, CuI, (triisopropylsilyl)acetylene, THF/NEt_3, r.t.; (c) $Pd(PPh_3)_4$, K_2CO_3, 4-pyridineboronic acid, THF/H_2O, 80 °C; (d) *n*-Bu_4NF, THF, r.t.; (e) $Pd(PPh_3)_4$, Ph4T-I, toluene, reflux; (f) $Pd(PPh_3)_4$, CuI, **2**, THF/*i*-Pr_2NEt, r.t.; (g) $PdCl_2(PPh_3)_2$, CuI, Ph4T-I, THF/NEt_3, r.t.

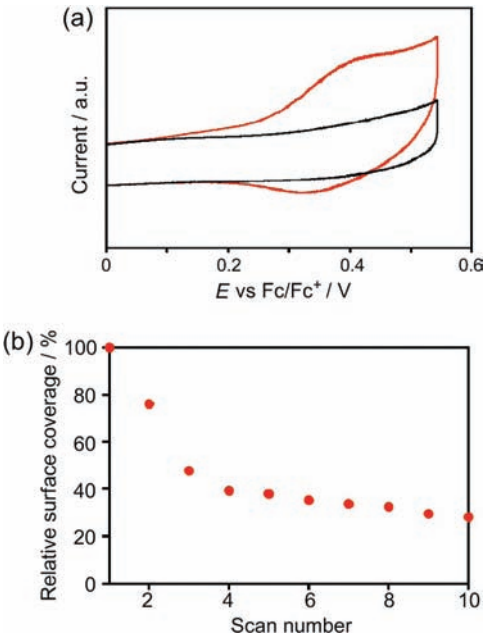

Figure 2. (a) CVs of **3Py-Ph4T**/Au (red) and **1Py-Ph4T**/Au (black). (b) Surface coverage as a function of the scan number.

adsorption via the π orbitals of the pyridine ring is favored for **3Py-TIPS**.

Conductance Measurements. Experiments for measuring the single-molecule conductance of **3Py-PE-3Py** were performed using a modified STM (Pico-SPM, Molecular Imaging Co.) with a Nano Scope IIIa controller (Digital Instruments Co.) in an electrochemical cell. Details of the experimental design used in this study have been previously reported by some of present authors.[25,26] The STM tip was made of an Au wire (diameter ~0.25 mm, purity >99%). The Au(111) substrate was prepared by the flame-annealing and quenching method. The solution of **3Py-PE-3Py** was adjusted to 0.2 mM in mesitylene. The STM tip was repeatedly moved into and out of contact with the substrate at a rate of 50 nm s^{-1} in the solution. The conductance was measured during the breaking process under an applied bias of 20 mV between the tip and substrate. All statistical data were obtained from a large number (over 1000) of individual conductance traces. The experiments were performed for three independent samples.

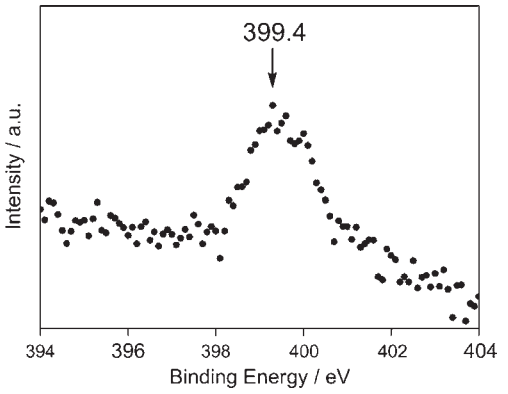

Figure 3. XPS spectrum of **3Py-TIPS** on gold.

Figure 4 shows the typical conductance traces and histograms of the Au point contacts in solutions with and without **3Py-PE-3Py**. In the solution containing **3Py-PE-3Py**, the conductance decreased in a stepwise fashion with each step occurring preferentially at an integer multiple of 5×10^{-4} G_0 (arrow in Figure 4(a)). Here, the G_0 is the unit of the conductance, $2e^2/h$, where e and h are the elementary electric charge and Planck's constant, respectively. The corresponding conductance histogram showed a distinctive feature at 5×10^{-4} G_0. Neither plateau nor any significant features were observed below 2×10^{-4} G_0 in the conductance traces and conductance histograms, respectively. In the solution without the molecules, neither plateaus nor peaks were observed in the conductance traces and conductance histograms. These experimental results indicate that the plateaus in the conductance traces and the distinctive feature in the conductance histogram, both of which occur at 5×10^{-4} G_0, could be ascribed to the bridging of a single **3Py-PE-3Py** molecule between the Au electrodes. The conductance of the single-molecule junction was determined to be $5 \pm 1 \times 10^{-4}$ G_0 by statistical analysis of repeated measurements (more than 3000 times on three independent samples). It has been referred that the phenylene-ethynylene π-conjugated system having the pyridine anchor unit **5** showed a single-molecule conductance of 3.5×10^{-6} G_0 in the MCBJ setup (Chart 1).[14] Compared to this molecule, **3Py-PE-3Py** showed a conductance larger by 2 orders of magnitude despite its longer molecular length. Furthermore, the conductance measurement of the contact created by a single pyridine anchor (**1Py**) was carried out recently though the used spacer (CH_2 or phenyl) is shorter than the **PE**.[12h] The present

dx.doi.org/10.1021/ja109577f |*J. Am. Chem. Soc.* 2011, 133, 3014–3022

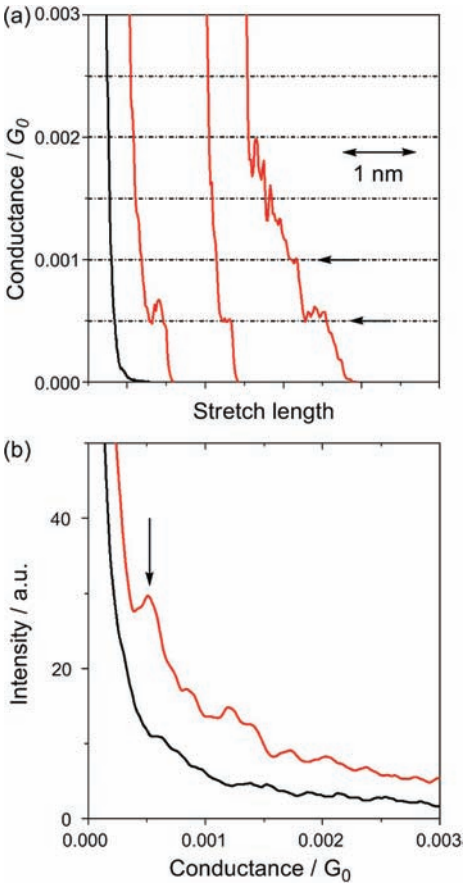

Figure 4. (a) Conductance traces measured when breaking the Au point contacts in solutions (red) with and (black) without **3Py-PE-3Py.** (b) Corresponding conductance histograms constructed without data selection from 1000 traces. Each histogram is normalized by the number of traces used to construct the histogram. The bin size is 10^{-5} G_0.

conductance is also larger by one (or two) orders of magnitude than the results given in ref 12h. This suggests effective hybridization of the metal electrode with the π orbital of the pyridine ring caused by **3Py** structure. In a later section, we check the validity of our consideration that the obtained conductance is provided by the contact of the **3Py** anchor, not by **1Py**, using ab initio calculations

Theoretical Analysis of Electric Transport. In order to analyze electron transport at the **3Py-PE-3Py** molecular junction, we performed ab initio calculations. A theoretical model of the junction was introduced according to the following procedures. First, we adopt two types of Au electrodes: clean Au(111) and Au(001) surfaces. This is because it is difficult to identify the rigorous structure of the electrode surfaces in the present experiments. An apex structure is often adopted in order to model devices created by break junctions for a single pyridine anchor.[12h,15k] However, we did not use the apex model in order to avoid an arbitrary conformation of the tripodal leg, as the conformation depends more strongly on the positions of apexes than in the case of a single-point anchor. Instead, we analyze the effects of varying the adsorption structures by adopting two clean surface structures as the theoretical model. We started from two kinds of structures, where one is constructed by the $p(6 \times 6)$ (111) and the other by $5\sqrt{2} \times 5\sqrt{2}$ (001) unit cell electrodes. The atomic positions in the **3Py-PE-3Py** were then

Chart 1. Chemical Structures and Conductances

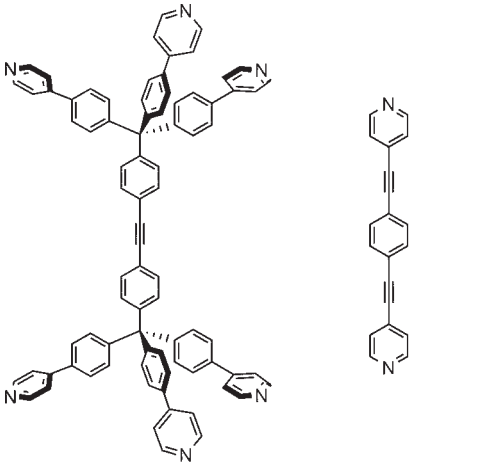

energetically optimized by the following procedure. First, we searched the adsorbed structure of the surface system, which consists of the **3Py-PE-3Py** and only a left side electrode. Using the obtained molecular conformation, we attached the electrode on the opposite side as a right side electrode. Then we performed the geometry optimization with relaxing **3Py-PE-3Py** and Au atoms of the top layers. We carried out this optimization with changing the distance between the left and right electrodes. Then we checked the total energy as the function of the distance. The adopted model junctions for the transport calculation give the minimum energy in the above procedures for (111) and (001) electrodes. We denote the resulting two junction models as "**3Py-PE-3Py**(111)" and "**3Py-PE-3Py**(001)."

The electronic structure calculations were performed by density functional theory (DFT) using the SIESTA package.[27] Transport calculations were then carried out by the nonequilibrium Green function technique combined with DFT (NEGF-DFT).[28] The conductance can be represented as $G_0T(E_F)$, where E_F is the Fermi level of the entire (semi-infinite) system and the transmission coefficient $T(E)$ is calculated by Green's function $G(E)$ and relevant lead self-energy terms. All of the NEGF calculations were performed by the HiRUNE module program,[29,30] developed by the one of the authors and implemented in SIESTA. To analyze the transport properties, we estimated the projected molecular orbitals (PMOs), where a PMO is defined as the eigenstate of the Hamiltonian projected onto the molecular region and the relevant eigenenergy is denoted as $E_\alpha{}^0$. The actual PMO energy shifts by Δ from $E_\alpha{}^0$ (i.e., $E_\alpha = E_\alpha{}^0 + \Delta$) and has an imaginary part γ because of coupling with the electrodes. The term γ relates to the molecule−electrode coupling strength. They can be strictly defined for each PMO Ψ_α using renormalized Green functions.[31] Hereafter, we label PMOs using standard terminologies: HOMO (highest occupied molecular orbital), LUMO (lowest unoccupied molecular orbital), etc., where the terminology of "HOMO/LUMO" is defined by the energy level E_α relative to E_F.

The structures of the device region obtained by DFT optimization are shown in Figure 5 as well as a few distinctive angles.

dx.doi.org/10.1021/ja109577f |J. Am. Chem. Soc. 2011, 133, 3014–3022

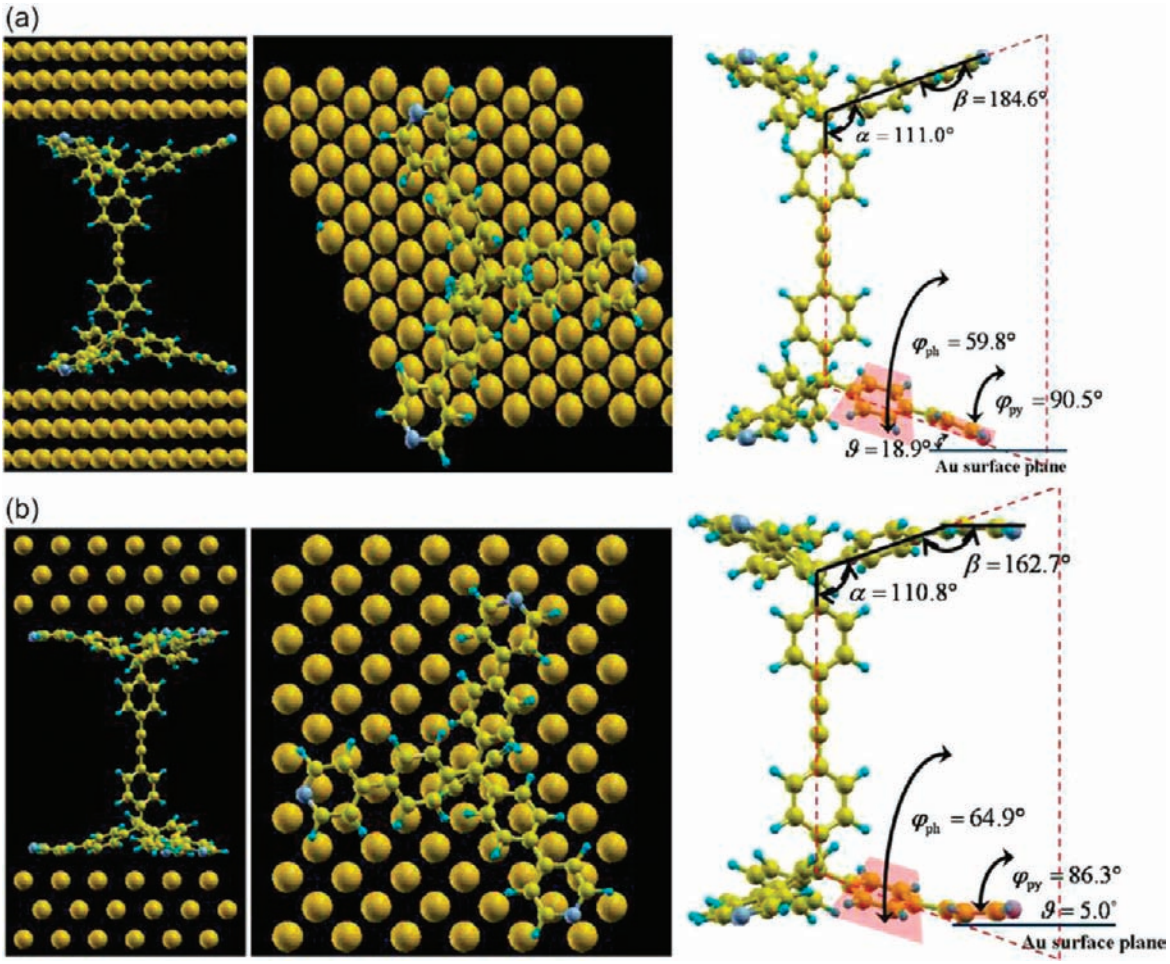

Figure 5. Structure of junctions adopted for the ab initio transport calculations. (a) **3Py-PE-3Py**(111) model and (b) **3Py-PE-3Py**(001) model, respectively. The left panels show side views of each system, whereas the middle panels show views from the top. The right panels give the details of the parameters to identify the conformations for **3Py**, such as dihedral and bending angles.

The three pyridine legs of **3Py-PE-3Py**(111) are anchored by the point contact between each N atom and metal. The tilt angle ϑ between the pyridine molecular plane and the Au surface is about 18.9° and each N atom is placed close to the on-top site while it slightly shifts in the hollow direction. The p orbital, which relates to the lone pair of N, connects to the electrode to form the contact. A little hybridization of the other p orbitals makes the π^* tilt slightly toward the molecular plane of the pyridine. In contrast, the pyridine rings of each leg of **3Py-PE-3Py**(001) lie on the Au surface, and their tilt angles ϑ are smaller than 5.0°. In particular, the pyridine plane for one of the three legs is almost parallel to the surface. Therefore, sufficient hybridization may occur between the metal and π state delocalized on the pyridine ring, where such a π contact potentially leads to charge donation and high conductance. When a reference plane (dotted line part in Figure 5) is defined as the plane consisted of the C_3-axis and a pointed N atom of **3Py**, the dihedral angles of the phenyl (φ_{ph}) and the pyridine (φ_{py}) in **3Py** are 64.9° and 86.3°, respectively. We also defined the bending angles α and β (see Figure 5). The angle β between the axis of the phenyl and pyridine is 162.7°, and the loss of energy by bending is compensated by the adsorption energy. Note that the legs of the tripodal anchor, particularly, of **3Py-PE-3Py**(001), were not equivalently connected to the electrodes in the present calculations. This is quite reasonable because not all subparts of the (001) surface can satisfy C_3 symmetry.

Table 1. Summary of the Calculated Conductance and Relevant PMOs for the 3Py-PE-3Py(111) and (001) Systems

model	conductance	PMO[a]	E_α (eV)[a]	γ (eV)	PDOS[b]
(111)	$1.16 \times 10^{-6}\ G_0$	HOMO	−1.97	−0.005	—
		LUMO	0.78	−0.046	0.36
(001)	$2.27 \times 10^{-4}\ G_0$	HOMO	−1.87	−0.016	—
		LUMO	0.64	−0.071	3.40

[a] Definitions of the PMO energy E_α and molecule-lead coupling γ are given in the text. Here we set the Fermi level to 0. [b] The PDOS is the value at the Fermi level. The value of HOMO is lower than 1.0×10^{-4} for both models.

The calculated conductance for **3Py-PE-3Py**(111) and (001) are $1.16 \times 10^{-6}\ G_0$ and $2.27 \times 10^{-4}\ G_0$, respectively, as shown in Table 1. The conductance depends on the surface Miller index of the electrode, which in turn strongly depends on the orientations of the attached pyridine as expected. The (001) electrode is far more electrically conductive than the (111) electrode. As stated above, there are potential differences in the electronic features of the π contact between **3Py-PE-3Py**(001) and (111). Therefore, it is worthwhile to compare the transport mechanisms of the two

dx.doi.org/10.1021/ja109577f |J. Am. Chem. Soc. 2011, 133, 3014–3022

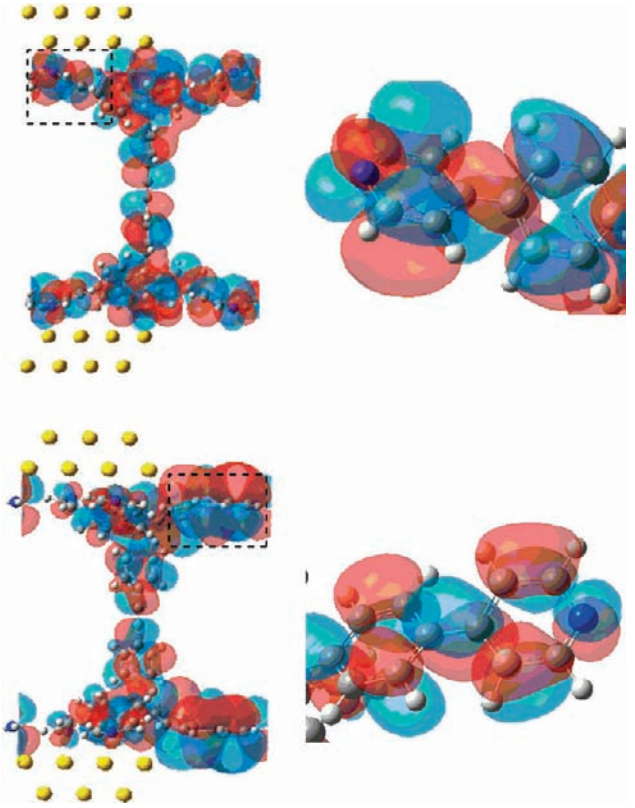

Figure 6. Plots of LUMO wave functions for **3Py-PE-3Py**(111) (upper left panel) and **3Py-PE-3Py**(001) (lower left panel), respectively. Each box of dashed lines represents the pyridine part of the wave function relevant to anchoring. Right panels show enlarged views of each boxed region.

model junctions. The calculated PMOs and relevant couplings are listed in Table 1. For both **3Py-PE-3Py**(111) and (001), the difference between the LUMO energy and E_F is much closer (1−1.2 eV) than that between the HOMO energy and E_F; thus, LUMO should dominate the transport. Furthermore, the molecule-lead coupling, γ, has a nonzero value for LUMO. As a result, we concluded that the conductive orbital is LUMO, and the transport carrier is an electron (electron transport) for each system.

To proceed with the analysis, we plotted the LUMO wave functions in Figure 6. The pyridine parts in LUMO are the π^* orbitals for both **3Py-PE-3Py**(111) and (001). However, the nodal planes of the p orbital of the N atom and the other delocalized π^* part of the pyridine are twisted around one another for **3Py-PE-3Py**(111). In contrast, the distribution of the wave function for LUMO of **3Py-PE-3Py**(001) is similar to that of a standard delocalized benzene π conjugate orbital, and the amplitude of the C−C π orbital overlaps with the metal. Using the PMO and Green's function, we calculated the projected density of states (PDOS) of (111) and (001) LUMO as a function of energy and found that the PDOS of LUMO for **3Py-PE-3Py**(001) are sufficiently large below E_F with a long tail: i.e., electron donation to π^* in the *tripodal* anchor is confirmed.

We emphasize that the (111) and (001) electrodes are only extremely idealized models: thus, the agreement of the conductances between the experimental and calculated values should be treated with a measure of caution. However, at the very least, the theoretical calculations support the experimental results, indicating that the formed **3Py-PE-3Py** could be sufficiently conductive. Furthermore, the transport mechanism itself, i.e., electron transport through the LUMO, is independent of electrode structure, although the conductance could be highly sensitive to the formed contact structure because of different types of pyridine−metal interactions.

Now, we examine the distinction between the tripodal anchor and single pyridine contact to show the consistency between the present experimental data and theoretical analysis. We performed additional transport calculations for **1Py-PE-1Py**(001), i.e., the unit **5** with (001) electrode (see Chart 1). Although we calculated several conformations of a single pyridine contact with the same procedures, the resulting conductance values were typically only ∼20% of **3Py-PE-3Py**(001). This value, 20%, is slightly large when the conductance by **1Py** anchoring reported previously is adopted.[14] However, the calculated conductance of **1Py** is sufficiently small compared with both the calculated (**3Py**) and the measured result. Hence, we conclude that the tripodal anchoring is essential to provide the present high conductance. Finally, we briefly comment on the use of GGA level DFT in the present NEGF framework. There are a few "beyond-DFT" transport calculations for the pyridine type systems, and their results improve the absolute values of conductance.[12h,13] However most of the calculations are based on only the partial correction scheme such as the GW correction for the bridge molecular part. According to several calculations of similar pyridine systems by NEGF-DFT,[12f,12i,12j] the use of GGA level is sufficient qualitatively for the present purpose to discuss the transport mechanism.

■ CONCLUSION

We have designed a new tripodal pyridine anchor to realize robust contact with metal electrodes and to achieve effective hybridization of the pyridine π orbital with metal electrodes. We successfully synthesized a series of tripodal pyridine-containing molecules. CV measurements of their monolayers on gold revealed that the tripodal structure has a great advantage in adsorption tendency compared to a single pyridine contact and in robustness even under biased conditions. These features can be explained by the multiplier effect of the tripodal pyridine anchor. As expected, XPS measurement indicated that the π orbital of pyridine contributes to the physical adsorption of our developed tripodal anchor on gold. Measurement of single-molecule conductance was successfully carried out using modified STM techniques for the phenylene-ethynylene chain connected with the present anchors. To our best knowledge, this is the first example wherein the electrical conductance for single-molecule bearing tripodal anchoring groups has been measured. The obtained conductance of $5 \pm 1 \times 10^{-4}$ G_0 is substantially higher than that of previously reported shorter π-conjugated chains with single-pyridine anchors. This result suggests that effective hybridization occurred as expected. Theoretical analysis based on ab initio calculations clearly supported the experimental results and our hypothesis of π channel conductance. The calculated results indicate an electron-transport mechanism for the present conduction system in which the LUMO dominates the transport. In pyridine-based tripodal anchoring, the π^* orbital of the pyridine part could directly interact with the electrode. Again, we emphasize our theoretical prediction that the above effective π contact enhances the conductance. The formation of the effective channel is caused by the adsorption structure of the

pointed pyridine, and anchoring by the tripodal moiety plays an important role to realize higher conductance than by a single atomic/molecular anchor. Therefore, we conclude that our newly developed tripodal pyridine anchor has opened the door to new strategies for achieving an ideal metal−molecular junction. We are now in the process of demonstrating this concept by investigating the dependence of conductance on the molecular length, the results of which will be reported in due course.

EXPERIMENTAL SECTION

General Information. Column chromatography was performed on silica gel, KANTO Chemical silica gel 60N (40−50 μm). TLC plates were visualized with UV light. Preparative gel-permeation chromatography (GPC) was performed on Japan Analytical Industry LC-908 equipped with JAI-GEL 1H/2H columns. Melting points are uncorrected. ^{1}H and ^{13}C NMR spectra were recorded on a JEOL JMN-400 spectrometer in $CDCl_3$ with tetramethylsilane as an internal standard. Data are reported as follows: chemical shift in ppm (δ), multiplicity (s = singlet, d = doublet, t = triplet, m = multiplet), coupling constant (Hz), and integration. Mass spectra were obtained on Shimadzu AXIMA-TOF. Cyclic voltammetry was carried out on a BAS ALC 620C voltammetric analyzer. Elemental analyses were performed on Perkin-Elmer LS-50B by the Elemental Analysis Section of Comprehensive Analysis Center (CAC), the Institute of Scientific and Industrial Research (ISIR), Osaka University. In the XPS measurement, Al Kα (1486.6 eV) and Mg Kα (1253.6 eV) were used as X-ray source. The calibration of binding energy was carried out with the peak of Au $4f_{7/2}$ at 84.0 eV as an energy reference.

Materials. All reactions were carried out under a nitrogen atmosphere. Solvents of the highest purity grade were used as received. Unless stated otherwise, all reagents were purchased from commercial sources and used without purification. 4-Trityliodobenzene (**1**)[32] and Ph4T[33] were prepared by reported procedures, and ^{1}H NMR data of these compounds were in agreement with those previously reported.

Synthesis of ***2***. Compound **1** (7.89 g, 17.7 mmol) was placed in a 500 mL round-bottomed flask and dissolved with dichloromethane (180 mL). To the mixture was added bromine (90.7 mL, 1.77 mmol) at 0 °C. The mixture was gradually warmed up to room temperature. After being stirred for 12 h, the mixture was added to satd $Na_2S_2O_3$ aq, and the organic layer was separated. The aqueous layer was extracted with dichloromethane, and the combined organic layer was washed with brine and dried over Na_2SO_4. After removal of the solvent under reduced pressure, the residue was washed by hexane and methanol to give **3** (10.2 g, 84%). White solid; >300 °C; ^{1}H NMR ($CDCl_3$) δ 6.88 (d, J = 8.7 Hz, 2H), 7.01 (d, J = 8.7 Hz, 6H), 7.39 (d, J = 8.7 Hz, 6H), 7.59 (d, J = 8.7 Hz, 2H); ^{13}C NMR ($CDCl_3$) δ 63.9, 92.5, 120.9, 131.2, 132.4, 132.7, 137.2, 144.5, 145.3; MS (MALDI-TOF, 1,8,9-trihydrioxyanthracene matrix) m/z 678.85 (M^+, calcd 679.78). Anal. Calcd for $C_{25}H_{16}Br_3I$: C, 43.96; H, 2.36; Found: C, 43.60; H, 2.00.

Synthesis of ***3***. Compound **2** (6.40 g, 9.37 mmol), $PdCl_2(PPh_3)_2$ (329 mg, 0.469 mmol), and CuI (89 mg, 0.467 mmol) were placed in a 2 L round-bottomed flask and dissolved with THF (300 mL) and triethylamine (300 mL). To the mixture was added (triisopropylsilyl)-acetylene (4.15 mL, 18.7 mmol) at 0 °C. The mixture was gradually warmed up to room temperature. After being stirred for 12 h, the reaction mixture was passed through Celite. After removal of the solvent under reduced pressure, the residue was purified by column chromatography on silica gel (hexane) to give **3** (6.32 g, 91%). White solid; mp 239−241 °C; ^{1}H NMR ($CDCl_3$) δ 1.18 (s, 21H), 7.02 (d, J = 8.9 Hz, 6H), 7.07 (d, J = 8.7, 2H), 7.36−7.39 (m, 8H); ^{13}C NMR ($CDCl_3$) δ 11.3, 18.6, 64.0, 91.4, 106.4, 120.7, 121.8, 130.5, 131.0, 131.6, 132.4, 144.5, 145.5; MS (MALDI-TOF, 1,8,9-trihydroxyanthracene matrix) m/z 734.78 (M^+, calcd 734.02). Anal. Calcd for $C_{36}H_{37}Br_3Si$: C, 58.63; H, 5.06; Found: C, 58.38; H, 4.86.

Synthesis of ***3Py-TIPS***. Compound **3** (800 mg, 1.08 mmol), 4-pyridineboronic acid (797 mg, 6.48 mmol), K_2CO_3 (1.19 g, 8.64 mmol), and $Pd(PPh_3)_4$ (125 mg, 0.108 mmol) were placed in a 200 mL round-bottomed flask and dissolved with THF (50 mL) and water (10 mL). The reaction mixture was stirred at 80 °C for 12 h. After being stirred for 12 h, the reaction was quenched by addition of water, and the organic layer was separated. The aqueous layer was extracted with EtOAc, and the combined organic layer was washed with brine and dried over Na_2SO_4. After removal of the solvent under reduced pressure, the residue was purified by column chromatography on silica gel (EtOAc/MeOH = 9/1) to give **3Py-TIPS** (647 mg, 82%). White solid; mp 227−229 °C; ^{1}H NMR ($CDCl_3$) δ 1.12 (s, 21H), 7.27 (d, J = 8.4 Hz, 2H), 7.41 (d, J = 8.2 Hz, 6H), 7.45 (d, J = 8.4 Hz, 2H), 7.51 (d, J = 4.8 Hz, 6H), 7.59 (d, J = 8.4 Hz, 6H), 8.66 (d, J = 4.8 Hz, 6H); ^{13}C NMR ($CDCl_3$) δ 11.3, 18.7, 64.6, 91.3, 106.6, 121.4, 121.7, 126.5, 130.7, 131.6, 131.6, 136.0, 146.1, 146.9, 147.4, 150.3; MS (MALDI-TOF, 1,8,9-trihydroxyanthracene matrix) m/z 732.14 (M^+, calcd 731.37). Anal. Calcd for $C_{51}H_{49}N_3Si$: C, 83.68; H, 6.75; N, 5.74; Found: C, 83.31; H, 6.87; N, 5.75.

Synthesis of ***Ph4T-I***. Ph4T (451 mg, 0.784 mmol) was placed in a 100 mL three-necked round-bottomed flask and dissolved with THF (20 mL). To the mixture was added *n*-BuLi (1.6 M hexane solution, 0.59 mL, 0.94 mmol) at −78 °C. After the mixture was stirred for 30 min at −78 °C, I_2 (299 mg, 1.18 mmol) was added. The mixture was gradually warmed to room temperature. After being stirred for 30 min, the reaction was quenched by addition of satd $Na_2S_2O_3$ aq, and the organic layer was separated. The aqueous layer was extracted with hexane, and the combined organic layer was washed with brine and dried over Na_2SO_4. After removal of the solvent under reduced pressure, the residue was purified by column chromatography on silica gel (hexane) to give **Ph4T-I** (520 mg, 95%). Yellow solid; mp 61−63 °C; ^{1}H NMR ($CDCl_3$) δ 0.87−0.92 (m, 6H), 1.25−1.48 (m, 12H), 1.56−1.75 (m, 4H), 2.73 (t, J = 8.1 Hz, 2H), 2.80 (t, J = 8.1 Hz, 2H), 6.97 (d, J = 3.7 Hz, 1H), 7.06 (d, J = 3.7 Hz, 1H), 7.08 (s, 1H), 7.12 (d, J = 3.7 Hz, 1H), 7.14 (d, J = 3.7 Hz, 1H), 7.17 (s, 1H), 7.28−7.30 (m, 1H), 7.36−7.40 (m, 2H), 7.59−7.61 (m, 2H); ^{13}C NMR ($CDCl_3$) δ 14.1, 14.1, 22.6, 22.6, 29.0, 29.1, 29.3, 29.6, 30.6, 30.6, 31.6, 31.7, 71.8, 123.8, 124.1, 125.6, 126.2, 126.3, 127.0, 127.6, 128.9, 129.8, 133.8, 134.0, 135.6, 136.3, 136.4, 137.4, 139.8, 140.8, 141.7, 142.1; MS (MALDI-TOF, 1,8,9-trihydroxyanthracene matrix) m/z 700.92 (M^+, calcd 700.08). Anal. Calcd for $C_{34}H_{37}IS_4$: C, 58.27; H, 5.32; Found: C, 58.16; H, 5.23.

Synthesis of ***3Py-Ph4T***. **3Py-TIPS** (349 mg, 0.48 mmol) was placed in a 100 mL round-bottomed flask and dissolved with THF (50 mL). To the mixture was added nBu$_4$NF (1.0 M THF solution, 0.95 mL, 0.95 mmol), and the mixture was stirred at room temperature for 30 min. The reaction was quenched by addition of satd $NaHCO_3$ aq, and the organic layer was separated. The aqueous layer was extracted with EtOAc, and the combined organic layer was washed with brine and dried over Na_2SO_4. After removal of the solvent under reduced pressure, the residue was used for the next reaction without further purification.

The residue, Ph4T-I (401 mg, 0.57 mmol), $PdCl_2(PPh_3)_2$ (33 mg, 0.048 mmol), and CuI (9 mg, 0.047 mmol) were placed in a 200 mL round-bottom flask and dissolved with THF (50 mL) and triethylamine (10 mL). The reaction mixture was stirred at room temperature. After being stirred for 12 h, the reaction mixture was passed through Celite. After removal of the solvent under reduced pressure, the residue was purified by column chromatography on silica gel (EtOAc/MeOH = 9/1) to give **3Py-Ph4T** (286 mg, 52% (two steps)). Yellow solid; mp 209−211 °C; ^{1}H NMR ($CDCl_3$) δ 0.90 (t, J = 7.1 Hz, 6H), 1.29−1.50 (m, 12H), 1.56−1.68 (m, 4H), 2.74−2.82 (m, 4H), 7.06 (d, J = 4.1 Hz, 1H), 7.07 (d, J = 4.1 Hz, 1H), 7.11 (s, 1H), 7.14 (d, J = 4.1 Hz, 1H), 7.15 (d, J = 4.1 Hz, 1H), 7.16 (s, 1H), 7.27−7.32 (m, 3H), 7.35−7.43 (m, 8H), 7.46

(d, J = 8.7 Hz, 2H), 7.54−7.63 (m, 14H), 8.66 (d, J = 6.4 Hz, 6H); ^{13}C NMR ($CDCl_3$) δ 14.1, 22.6, 29.2, 29.3, 29.3, 29.6, 30.4, 30.5, 31.7, 31.7, 64.6, 83.3, 93.6, 120.8, 121.1, 123.9, 124.1, 125.5, 126.2, 126.3, 126.5, 126.9, 127.6, 128.9, 129.8, 130.9, 130.9, 131.6, 132.5, 133.9, 134.2, 135.1, 135.6, 136.0, 136.3, 137.3, 139.7, 40.8, 142.1, 142.6, 146.9, 147.4, 150.0; MS (MALDI-TOF, 1,8,9-trihydroxyanthracene matrix) m/z 1147.84 (M^+, calcd 1147.41); Anal. Calcd for $C_{76}H_{65}N_3S_4$: C, 79.47; H, 5.70; N, 3.66; Found: C, 79.31; H, 5.61; N, 3.43.

Synthesis of ***3Py-PE-3Py***. **3Py-TIPS** (83 mg, 0.11 mmol) was placed in a 100 mL round-bottomed flask and dissolved with THF (20 mL). To the mixture was added nBu$_4$NF (1.0 M THF solution, 0.22 mL, 0.23 mmol), and the mixture was stirred at room temperature for 30 min. The reaction was quenched by addition of satd $NaHCO_3$ aq, and the organic layer was separated. The aqueous layer was extracted with hexane, and the combined organic layer was washed with brine and dried over Na_2SO_4. After removal of the solvent under reduced pressure, the residue was used for the next reaction without further purification.

The residue, **2** (116 mg, 0.17 mmol), $Pd(PPh_3)_4$ (13 mg, 0.011 mmol), and CuI (2 mg, 0.011 mmol) were placed in a 30 mL round-bottom flask and dissolved with THF (6 mL) and iPr$_2$NEt (2 mL). The reaction mixture was stirred at room temperature for 12 h. After removal of the solvent under reduced pressure, the residue was purified by column chromatography on silica gel (EtOAc/MeOH/Et_3N = 18/1/1) to give compound **A** (75 mg, 58% (two steps)). White solid; mp 132−134 °C; ^{1}H NMR ($CDCl_3$) δ 7.03 (d, J = 8.8 Hz, 6H), 7.12 (d, J = 8.3 Hz, 2H), 7.30 (d, J = 8.3 Hz, 2H), 7.37−7.45 (m, 14H), 7.48 (d, J = 8.8 Hz, 2H), 7.51 (d, J = 6.1 Hz, 6H), 7.61 (d, J = 8.8 Hz, 6H), 8.66 (d, J = 6.1 Hz, 6H); MS (MALDI-TOF, 1,8,9-trihydroxyanthracene matrix) m/z 1127.98 (M^+, calcd 1127.11).

Compound **A** (55 mg, 0.049 mmol), 4-pyridineboronic acid (36 mg, 0.29 mmol), K_2CO_3 (54 mg, 0.39 mmol), and $Pd(PPh_3)_4$ (17 mg, 0.015 mmol) were placed in a test tube and dissolved with THF (5 mL) and water (1 mL). The reaction mixture was stirred at 80 °C for 12 h. The reaction mixture was extracted with hexane and the organic layer was washed with brine and dried over Na_2SO_4. After removal of the solvent under reduced pressure, the residue was purified by column chromatography on alumina ($CHCl_3$/MeOH = 9/1) to give **3Py-PE-3Py** (49 mg, 90%). White solid; mp >300 °C; ^{1}H NMR ($CDCl_3$) δ 7.28 (d, J = 8.8 Hz, 4H), 7.41 (d, J = 8.5 Hz, 12H), 7.46−7.53 (m, 16H), 7.60 (d, J = 8.5 Hz, 12H), 8.66 (d, J = 6.4 Hz, 12H); MS (MALDI-TOF, 1,8,9-trihydroxyanthracene matrix) m/z 1123.78 (M^+, calcd 1124.46). Anal. Calcd for $C_{82}H_{56}N_6$: C, 87.52; H, 5.02; N, 7.47; Found: C, 87.80; H, 5.07; N, 7.19.

Synthesis of ***1Py-Ph4T***. 4-Ethynylpyridine (**4**) (55 mg, 0.53 mmol), Ph4T-I (308 mg, 0.44 mmol), $PdCl_2(PPh_3)_2$ (31 mg, 0.044 mmol), and CuI (8 mg, 0.042 mmol) were placed in a 50 mL round-bottom flask and dissolved with THF (21 mL) and Et_3N (7 mL). The reaction mixture was stirred at room temperature for 12 h. After removal of the solvent under reduced pressure, the residue was purified by column chromatography on silica gel (hexane/EtOAc = 3/1) to give **1Py-Ph4T** (59 mg, 20%). Black oil; ^{1}H NMR ($CDCl_3$) δ 0.90 (t, J = 7.1 Hz, 6H), 1.22−1.50 (m, 12H), 1.56−1.68 (m, 4H), 2.75−2.82 (m, 4H), 7.07 (d, J = 4.1 Hz, 1H), 7.15−7.17 (m, 3H), 7.19 (s, 1H), 7.27−7.33 (m, 1H), 7.34−7.41 (m, 4H), 7.60 (d, J = 7.4 Hz, 2H), 8.60 (d, J = 6.4 Hz, 2H); ^{13}C NMR ($CDCl_3$) δ 14.1, 22.6, 22.6, 29.1, 29.3, 29.3, 29.6, 30.4, 30.5, 31.6, 31.7, 87.6, 91.4, 119.4, 123.9, 124.2, 125.0, 125.5, 126.1, 126.3, 127.2, 127.6, 128.9, 129.7, 131.1, 133.9, 133.9, 135.7, 136.2, 136.3, 137.7, 139.8, 140.8, 142.1, 149.7; MS (MALDI-TOF, 1,8,9-trihydroxyanthracene matrix) m/z 675.97 (M^+, calcd 675.21) ; Anal. Calcd for $C_{41}H_{41}NS_4$: C, 72.84; H, 6.11; N, 2.07; Found: C, 73.10; H, 6.08; N, 1.94.

■ ASSOCIATED CONTENT

Ⓢ Supporting Information. ^{1}H NMR spectra of **3Py-TIPS**, **3PY-Ph4T**, **1Py-Ph4T**, and **3Py-PE-3Py** as well as the cyclic voltammogram of **3Py-Ph4T**. Complete ref 1. This material is available free of charge via the Internet at http://pubs.acs.org

■ AUTHOR INFORMATION

Corresponding Author

hs-nakamura@aist.go.jp; kiguti@chem.titech.ac.jp; aso@sanken.osaka-u.ac.jp

■ ACKNOWLEDGMENT

The authors are grateful to T. Ohto (the University of Tokyo) for helpful discussions and support through calculations. This work was supported in part by Grants-in-Aids for Scientific Research on Priority Areas, "Electron Transport Through a Linked Molecule in Nano-Scale" (Grant No. 17069006) and Management Expenses Grants for National Universities Corporations from the Ministry of Education, Culture, Sports, Science, and Technology, Japan. Thanks are extended to the Elemental Analysis Section of the Comprehensive Analysis Center (CAC) of the Institute of Scientific and Industrial Research (ISIR), Osaka University, for assistance in obtaining elemental analyses.

■ REFERENCES

(1) Adams, D. M.; et al. *J. Phys. Chem. B* **2003**, *107*, 6668.

(2) Melosh, N.; Boukai, A.; Diana, F.; Gerardot, B.; Badolato, A.; Petroff, P.; Heath, J. R. *Science* **2003**, *300*, 112.

(3) Novoselov, K.; Geim, A. K.; Morozov, S. V.; Jiang., D.; Katsnelson, M. I.; Grigorieva, I. V.; Dubonos, S. V.; Firsov, A. A. *Nature* **2005**, *438*, 197.

(4) (a) Tao, N. J. *Nat. Nanotechnol.* **2006**, *1*, 173.(b) Cuevas, J. C.; Scheer, E. *Molecular Electronics: An Introduction to Theory and Experiment*; World Scientific: Singapore, 2010.

(5) Aviram, A.; Ratner, M. *Chem. Phys. Lett.* **1974**, *29*, 277.

(6) Reed, M. A.; Zhou, C.; Muller, C. J.; Burgin, T. P.; Tour, J. M. *Science* **1997**, *278*, 252.

(7) Xu, B.; Tao, N. J. *Science* **2003**, *301*, 1221.

(8) Chen, F.; Li, X.; Hihath, J.; Huang, Z.; Tao, N. *J. Am. Chem. Soc.* **2006**, *128*, 15874.

(9) (a) Patrone, L.; Palacin, S.; Bourgoin, J. P. *Appl. Surf. Sci.* **2003**, *212*−*213*, 446. (b) Patrone, L.; Palacin, S.; Charlier, J.; Armand, F.; Bourgoin, J. P.; Tang, H.; Gauthier, S. *Phys. Rev. Lett.* **2003**, *91*, 096802/1. (c) Yasuda, S.; Yoshida, S.; Sasaki, J.; Okutsu, Y.; Nakamura, T.; Taninaka, A.; Takeuchi, O.; Shigekawa, H. *J. Am. Chem. Soc.* **2006**, *128*, 7746. (d) Yokota, K.; Taniguchi, M.; Kawai, T. *J. Am. Chem. Soc.* **2007**, *129*, 5818. (e) Yokota, K.; Taniguchi, M.; Tanaka, H.; Kawai, T. *Phys. Rev. B* **2008**, *77*, 165416/1.

(10) Ie, Y.; Hirose, T.; Yao, A.; Yamada, T.; Takagi, N.; Kawai, M.; Aso, Y. *Phys. Chem. Chem. Phys.* **2009**, *11*, 4949.

(11) (a) Venkataraman, L.; Klare, J. E.; Tam, I. W.; Nuckolls, C.; Hybertsen, M. S.; Steigerwald, M. L. *Nano Lett.* **2006**, *6*, 458. (b) Quinn, J. R.; Foss, F. W., Jr.; Venkataraman, L.; Hybertsen, M. S.; Breslow, R. *J. Am. Chem. Soc.* **2007**, *129*, 6714. (c) Venkataraman, L.; Park, Y. S.; Whalley, A. C.; Nuckolls, C.; Hybertsen, M. S.; Steigerwald, M. L. *Nano Lett.* **2007**, *7*, 502.

(12) (a) Xu, B.; Xiao, X.; Tao, N. J. *J. Am. Chem. Soc.* **2003**, *125*, 16164. (b) Li, X.; Hihath, J.; Chen, F.; Masuda, T.; Zang, L.; Tao, N. *J. Am. Chem. Soc.* **2007**, *129*, 11535. (c) Li, C.; Mishchenko, A.; Li, Z.; Pobelov, I.; Wandlowski, T.; Li, X. Q.; Würthner, F.; Bagrets, A.; Evers, F. *J. Phys., Condens. Matter.* **2008**, *20*, 374122. (d) Zhou, X.-S.; Chen, Z.-B.; Liu, S.-H.; Jin, S.; Liu, L.; Zhang, H.-M.; Xie, Z.-X.; Jiang, Y.-B.; Mao, B.-W. *J. Phys. Chem. C* **2008**, *112*, 3935. (e) Horiguchi, K.; Kurokawa, S.; Sakai, A. *J. Chem. Phys.* **2009**, *131*, 104703. (f) Wang, C.; Batsanov, A. S.; Bryce, M. R.; Martin, S.; Nichols, R. J.; Higgins, S. J.; Garcia-Suárez, V. M.; Lambert, C. J. *J. Am. Chem. Soc.* **2009**, *131*, 15647.

(g) Pan, S.; Zhao, A.; Wang, B.; Yang, J.; Hou, J. *Adv. Mater.* **2010**, *22*, 1967. (h) Kamenetska, M.; Quek, S. Y.; Whalley, A. C.; Steigerwald, M. L.; Choi, H. J.; Louie, S. G.; Nuckolls, C.; Hybertsen, M. S.; Neaton, J. B.; Venkataraman, L. *J. Am. Chem. Soc.* **2010**, *132*, 6817. (i) Stadler, R. *Phys. Rev. B* **2010**, *81*, 165429. (j) Garcia-Suárez, V. M.; Lambert, C. J. *Nanotechnology* **2008**, *19*, 455203.

(13) Quek, S. Y.; Kamenetska, M.; Steigerwald, M. L.; Choi, H. J.; Louie, S. G.; Hybertsen, M. S.; Neaton, J. B.; Venkataraman, L. *Nat. Nanotechnol.* **2009**, *4*, 230.

(14) Grunder, S.; Huber, R.; Wu, S.; Schönenberger, C.; Calame, M.; Mayor, M. *Eur. J. Org. Chem.* **2010**, 833.

(15) (a) Bilić, A.; Reimers, J. R.; Hush, N. S. *J. Phys. Chem. B* **2002**, *106*, 6740. (b) Tada, T.; Kondo, M.; Yoshizawa, K. *J. Chem. Phys.* **2004**, *121*, 8050. (c) Stadler, R.; Thygesen, K. S.; Jacobsen, K. W. *Phys. Rev. B* **2005**, *72*, 241401-1. (d) Li, Q.; Wu, X.; Huang, J.; Yang, J. *Ultramicroscopy* **2005**, *105*, 293. (e) Wu, X.; Li, Q.; Huang, J.; Yang, J. *J. Chem. Phys.* **2005**, *123*, 184712. (f) Péréz-Jiménez, Á. J. *J. Phys. Chem. B* **2005**, *109*, 10052. (f) Stadler, R.; Jacobsen, K. W. *Phys. Rev. B* **2006**, *74*, 161405-1. (g) Hou, S.; Zhang, J.; Li, R.; Ning, J.; Han, R.; Shen, Z.; Zhao, X.; Xue, Z.; Wu, Q. *Nanotechnology* **2005**, *16*, 239. (h) Hou, S.; Ning, J.; Shen, Z.; Zhao, X.; Xue, Z. *Chem. Phys.* **2006**, *327*, 1. (i) Li, R.; Hou, S.; Zhang, J.; Qian, Z.; Shen, Z.; Zhao, X. *J. Chem. Phys.* **2006**, *125*, 194113. (j) Strange, M.; Kristensen, I. S.; Thygesen, K. S.; Jacobsen, K. W. *J. Chem. Phys.* **2008**, *128*, 114714. (k) Stadler, R. *Phys. Rev. B* **2010**, *81*, 165429-1.

(16) Kiguchi, M.; Tal, O.; Wohlthat, S.; Pauly, F.; Krieger, M.; Djukic, D.; Cuevas, J. C.; van Ruitenbeek, J. M. *Phys. Rev. Lett.* **2008**, *101*, 046801.

(17) (a) Martin, C. A.; Ding, D.; Sørensen, J. K.; Bjørnholm, T.; van Ruitenbeek, J. M.; van der Zant, H. S. J. *J. Am. Chem. Soc.* **2008**, *130*, 13198. (b) Kiguchi, M. *Appl. Phys. Lett.* **2009**, *95*, 073301.

(18) Pump, F.; Temirov, R.; Neucheva, O.; Soubatch, S.; Tautz, S.; Rohlfing, M.; Cuniberti, G. *Appl. Phys. A: Mater. Sci. Process.* **2008**, *98*, 335.

(19) (a) Whitesell, J. K.; Chang, H. K. *Science* **1993**, *261*, 73. (b) Fox, M. A.; Whitesell, J. K.; McKerrow, A. J. *Langmuir* **1998**, *14*, 816. (c) Yao, Y.; Tour, J. M. *J. Org. Chem.* **1999**, *64*, 1968. (d) Guo, W.; Galoppini, E.; Rydja, G.; Pardi, G. *Tetrahedron Lett.* **2000**, *41*, 7419. (e) Hu, J.; Mattern, D. L. *J. Org. Chem.* **2000**, *65*, 2277. (f) Jian, H.; Tour, J. M. *J. Org. Chem.* **2003**, *68*, 5091. (g) Yam, C. M.; Cho, J.; Cai, C. *Langmuir* **2003**, *19*, 6862. (h) Park, J.-S.; Vo, A. N.; Barriet, D.; Shon, Y.-S.; Lee, T. R. *Langmuir* **2005**, *21*, 2902. (i) Shirai, Y.; Cheng, L.; Chen, B.; Tour, J. M. *J. Am. Chem. Soc.* **2006**, *128*, 13479. (j) Kitagawa, T.; Idomoto, Y.; Matsubara, H.; Hobara, D.; Kakiuchi, T.; Okazaki, T.; Komatsu, K. *J. Org. Chem.* **2006**, *71*, 1362. (k) T. Weidner, T.; Krämer, A.; Bruhn, C.; Zharnikov, M.; Shaporenko, A.; Siemeling, U.; Träger, F. *Dalton Trans.* **2006**, 2767.

(20) (a) Galoppini, E.; Guo, W.; Qu, P.; Meyer, G. J. *J. Am. Chem. Soc.* **2001**, *123*, 4342. (b) Galoppini, E.; Guo, W.; Zhang, W.; Hoertz, P. G.; Qu, P.; Meyer, G. J. *J. Am. Chem. Soc.* **2002**, *124*, 7801. (c) Deng, X.; Mayeux, A.; Cai, C. *J. Org. Chem.* **2002**, *67*, 5279. (d) Deng, X.; Cai, C. *Tetrahedron Lett.* **2003**, *44*, 815. (e) Loewe, R. S.; Ambroise, A.; Muthukumaran, K.; Padmaja, K.; Lysenko, A. B.; Mathur, G.; Li, Q.; Bocian, D. F.; Misra, V.; Lindsey, J. S. *J. Org. Chem.* **2004**, *69*, 1453. (f) Yam, C. M.; Cho, J.; Cai, C. *Langmuir* **2004**, *20*, 1228. (g) Deluge, M.; Cai, C. *Langmuir* **2005**, *21*, 1917. (h) Thamyongkit, P.; Yu, L.; Padmaja, K.; Jiao, J.; Bocian, D. F.; Lindsey, J. S. *J. Org. Chem.* **2006**, *71*, 1156. (i) Quintiliani, M.; Kahnt, A.; Vázquez, P.; Guldi, D. M.; Torres, T. *J. Mater. Chem.* **2008**, *18*, 1542.

(21) (a) Zhu, L.; Tang, H.; Harima, Y.; Yamashita, K.; Hirayama, D.; Aso, Y.; Otsubo, T. *Chem. Commun.* **2001**, 1830. (b) Hirayama, D.; Takimiya, K.; Aso, Y.; Otsubo, T.; Hasobe, T.; Yamada, H.; Imahori, H.; Fukuzumi, S.; Sakata, Y. *J. Am. Chem. Soc.* **2002**, *124*, 532.

(22) (a) Wei, L.; Padmaja, K.; Youngblood, W. J.; Lysenko, A. B.; Lindsey, J. S.; Bocian, D. F. *J. Org. Chem.* **2004**, *69*, 1461. (b) Wei, L.; Tiznado, H.; Liu, G.; Padmaja, K.; Lindsey, J. S.; Zaera, F.; Roclan, D. F. *J. Phys. Chem. B* **2005**, *109*, 23963. (c) Sakata, T.; Maruyama, S.; Ueda, A.; Otsuka, H.; Miyahara, Y. *Langmuir* **2007**, *23*, 2269.

(23) Moulder, J. F.; Stickle, W. F.; Sobol, K. D.; Bomben, K. D.; Chastain King, Jr., J.; *Handbook of X-ray Photoelectron Spectroscopy*, 2nd ed.; Physical Electronics, Inc.: Eden Prairie, 1995.

(24) Behzadi, B.; Ferri, D.; Baiker, A.; Ernst, K.-H. *Appl. Surf. Sci.* **2007**, *253*, 3480.

(25) Kiguchi, M.; Miura, S.; Hara, K.; Sawamura, M.; Murakoshi, K. *Appl. Phys. Lett.* **2007**, *91*, 053110.

(26) Kiguchi, M.; Miura, S.; Takahashi, T.; Hara, K.; Sawamura, M.; Murakoshi, K. *J. Phys. Chem. C* **2008**, *112*, 13349.

(27) Soler, J. M.; Artacho, E.; Gale, J. D.; Garcia, A.; Junquera, J.; Ordejon, P.; Sanchez-Portal, D. *J. Phys.: Condens. Matter* **2002**, *14*, 2745.

(28) Brandbyge, M.; Mozos, J. L.; Ordejon, P.; Taylor, J.; Stokbro, K. *Phys. Rev. B* **2002**, *65*, 165401–1.

(29) Nakamura, H.; Yamashita, K. *J. Chem. Phys.* **2006**, *125*, 194106–1.

(30) Nakamura, H.; Yamashita, K.; Rocha, A. R.; Sanvito, S. *Phys. Rev. B* **2008**, *78*, 235420–1.

(31) Nakamura, H. *J. Phys. Chem. C* **2010**, *114*, 12280.

(32) Li, Q.; Rukavishnikov, A. V.; Petukhov, P. A.; Zaikova, T. O.; Keana, J. F. W. *Org. Lett.* **2002**, *4*, 3631.

(33) Negishi, N.; Ie, Y.; Taniguchi, M.; Kawai, T.; Tada, H.; Kaneda, T.; Aso, Y. *Org. Lett.* **2007**, *9*, 829.